Supplement of beyond 2D inventories: synoptic 3D landslide volume calculation from repeat LiDAR data

Thomas G. Bernard, Dimitri Lague, Philippe Steer

Géosciences Rennes, Rennes University, Rennes, 35042, France

S1. Analysis and selection of M3C2 parameter values

S1.1. Normal scale *D*

The normal scale *D* is a parameter that will influence the normal orientation along which the mean distance between the two point clouds will be computed. Lague et al., 2013, show how if D is too small with respect to the roughness of the surface, the mean distance between two point clouds is overestimated due to normal flickering. It is thus important to select a normal scale that (i) is not affected by the roughness surface and (ii) that is small enough to allow the detection of large scale changes in surface orientation like hilltop and bed and banks of the river. To determine the value of D, we followed the recommendation of Lague et al. (2013) that "*D* should be at least 20-25 times larger than the roughness σ(D)". The ratio between *D* and mean roughness (ζ) was thus computed for both the pre-earthquake and post-earthquake surfaces for different normal scale (Fig.S1 (a)). Results show that $\zeta > 25$ for both surfaces when $D > 5$m on average, but for the pre-EQ data which is of lower point density, we observe a plateau in the percentage of core points 85 % verifying this condition around 10 m. We thus choose D = 10 m to limit the roughness effect on normal calculation.

S1.2 Projection scale *d*

The M3C2 algorithm allows to compute 3D distance between two average positions of two different point clouds at a scale *d* (projection scale). In order to select the best projection scale *d*, we used the two random sub-sampled versions of the post-event point cloud described in the paper section 3.1. These two clouds represent exactly the same topographic surface with a different random sampling. As the two surfaces are identical, all change detection measurements should be statistically non-significant. The best projection scale *d* corresponds to the scale for which (i) change detection measurements are statistically non-significant, (ii) the number of points considered in the calculation of the statistics are sufficient and (iii) that is small enough to get the best spatial resolution of the 3D distance field, and limit smoothing of the signal. As the validity of eq. (2) was never tested on airborne lidar data, we thus analysed, for different projection scale d (from 1 m to 40 m), the percentage of non-significant points detected by the M3C2 algorithm and the percentage of points for which the level of detection (LoD) can be computed with at least 5 points. Results show that (Fig.S1 (b)): (i) when it can be computed the LoD actually predicts no significant change at least 95 of the time, indicating that the statistical model behind eq. (2) (Lague et al., 2013) is correct; (ii) the fraction of core points for which the LoD can be calculated rapidly increases between 1 and 8 m at which point it

reaches 100 %. Given that *d* largely sets the effective resolution of the 3D distance field, we aim at keeping it as small as possible to increase the capacity to detect very small landslides. We choose *d*=5 m as it represents a good balance between the ability to compute LoD on the majority of core points (here, ~ 97 %) and the smallest projection scale possible. We note that *d* could theoretically be set as a function of the lowest mean point density of the two LiDAR datasets, *res*, by $d \sim 2\sqrt{5/\pi res}$. In our case the pre-EQ dataset has *res* = 3.8 pts/m² and would predict *d* = 1.3 m. However, the presence of vegetation significantly reduces the ground point density in the lidar data and the overlapping of flight lines creates localized high point density that gives an incomplete picture of the actual distribution of points on the ground. For instance, despite having a mean point density *res* = 11.5 pts/m², that theoretically predicts *d* = 0.74 m, an optimal *d* for datasets having point distribution similar to the post-EQ dataset would probably be 3.5 m for which a LOD can be calculated for 98 % of the points. This highlights that higher point density does increase the effective resolution of our workflow, but that the penetration below vegetation and the actual distribution of points on the ground is an essential characteristic. One could consider using different values of *d* for bare surfaces and vegetated surfaces to increase the spatial resolution on the former one, but we have not explored this path yet.

The previous analysis shows that the mean point density can thus hardly be used as an indicator of the optimal *d*. The best practice to set *d*, once *D* and p_{max} have been selected, is to perform the 3D-M3C2 operation with various *d* using the actual lidar datasets, and identify the minimum projection scale for which the LoD can be calculated for a fraction of the core points as close as possible to 1.

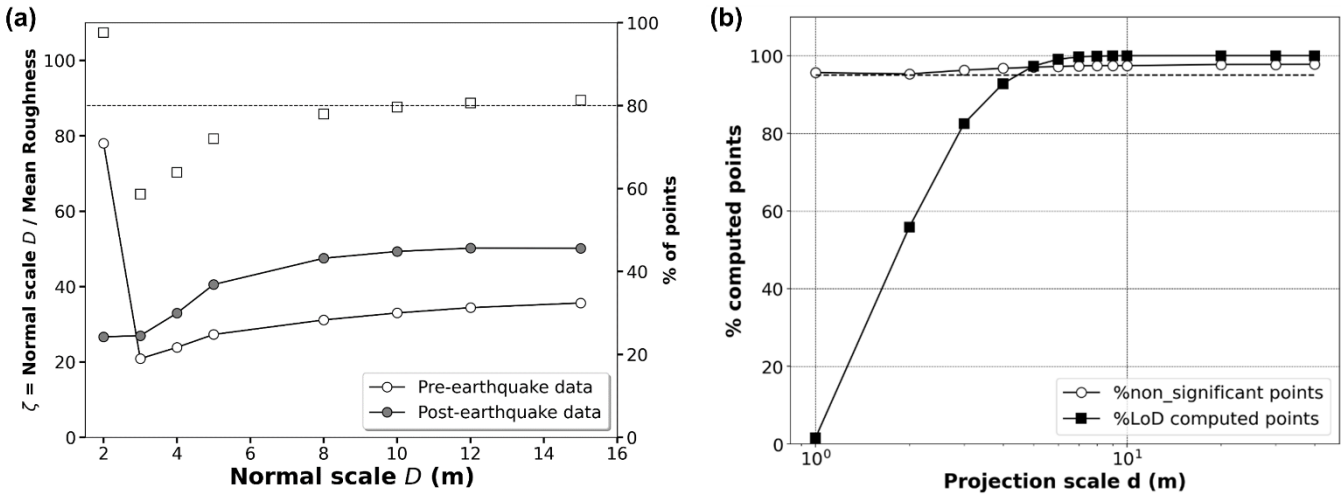

Fig.S1. Analysis of two main parameters of the M3C2 algorithm: the normal scale *D* and the projection scale *d*. (a) Ratio between normal scale and mean roughness for different normal scale value, and fraction of the pre-earthquake core points for which the normal scale is 25 times larger than the local roughness. (b) Percentage of computed points with a confidence interval of 95% versus projection scale d. The percentage of non-significant points is represented as well as the percentage of points where the Level of Detection (LoD) was computed (i.e., with at least 5 points on each point cloud).

S2. Detailed landslide detection workflow

S2.1. Registration

Table S2. Value of the transformation apply on the post-earthquake LiDAR data along the X, Y and Z axis.

	X	Y	Z
Coarse registration (m)	-	-	- 1.36
ICP fine registration (m)	-1.40	0.14	0.85

S2.2 Landslide segmentation by connected component

The individualization of landslides was performed by a connected component algorithm which is based on two criteria: a minimum distance D_m between two sub-clouds and a minimum number of points N_p defining these sub-clouds. The two next sub-sections detail the methodology used to determine the best value for these two parameters.

S2.2.1 Determination of the minimum number of points considered as landslide

The aim of the following analysis is to determine the minimum number of points considered in each sub-clouds for which we can be confident that it corresponds to a landslide. The landslide mapping workflow was first applied to the two random sub-sampled versions of the post-event point cloud presented in the section 3.1, and N_p was set to 1 during the segmentation step (i.e., the minimum landslide area is 1 core point, that is 1 m²). Given that the same surface is compared, the detected "landslides" are artefacts due to the different sampling of a rough surface. We compared the probability density distribution of the artefact areas with the distribution of the landslide areas detected from the comparison between the pre-earthquake and post-earthquake data using Np = 1(Fig. S.2.2.1). Results show that the area distribution of artefacts decreases as a power -2.95 while actual landslides resulting from the true data analysis decrease with an exponent – 1.87. Given the prevalence of artefacts for areas between 1 and 10 m², we cannot confidently assess whether a detected landslide is an artefact related to the sampling/roughness effect or a true landslide. However, for an area greater than 10 m² the probability of having an artefact significantly drops. In this study, we use a conservative minimum area of 20 m² as the minimum detectable landslide area, and a minimum number of core points N_p =20 was set during the segmentation process. Given that the probability of having artefacts and true landslides for 20 m² differs by two orders of magnitude, we are confident that the detected spatially coherent changes above that threshold area corresponds to real changes, and not artefacts.

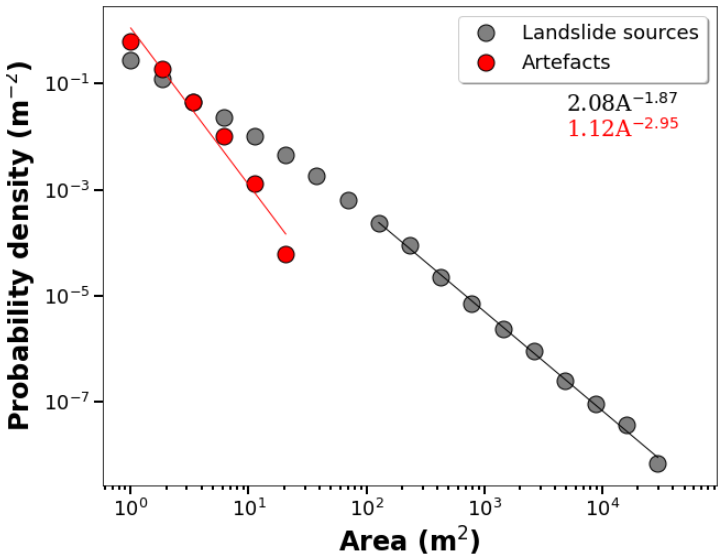

Figure S2.2.1: Comparison between the probability density distribution of detected artefacts (red) and landslide scars (gray).

S2.2.2 Sensitivity analysis of the minimum segmentation distance D_m between two sub-clouds

We performed an analysis of the impact of D_m on the resulting geometric characteristics of individual landslide source s using the same workflow as described in the paper. The resulting analysis is presented in figure S2.2.2 and table 2.2.2. Consistent with an increase of the amalgamation effect with D_m the exponents of the power-law scaling of the landslide area and landslide volume distributions tend to increase with D_m with a total number of landslides decreasing from 2083 (D_m = 1 m) to 406 (D_m = 8 m). Similarly, increasing D_m reduces the power-law exponent of the volume-area relationship from 1.22 to 1.13. Yet, these results show that the range of value of D_m explored here does not greatly affect the value of the power-law scaling parameters, although it has a significant impact on the total number of landslides. Because values of D_m < 4 m² tend to generate geometric properties that fall within the confidence interval of D_m = 2 m, while values greater than 4 m significantly deviate, we choose D_m =2 m. It also corresponds to the scale at which the amalgamation of the biggest landslides (> 500 m²) and the over-segmentation appears limited.

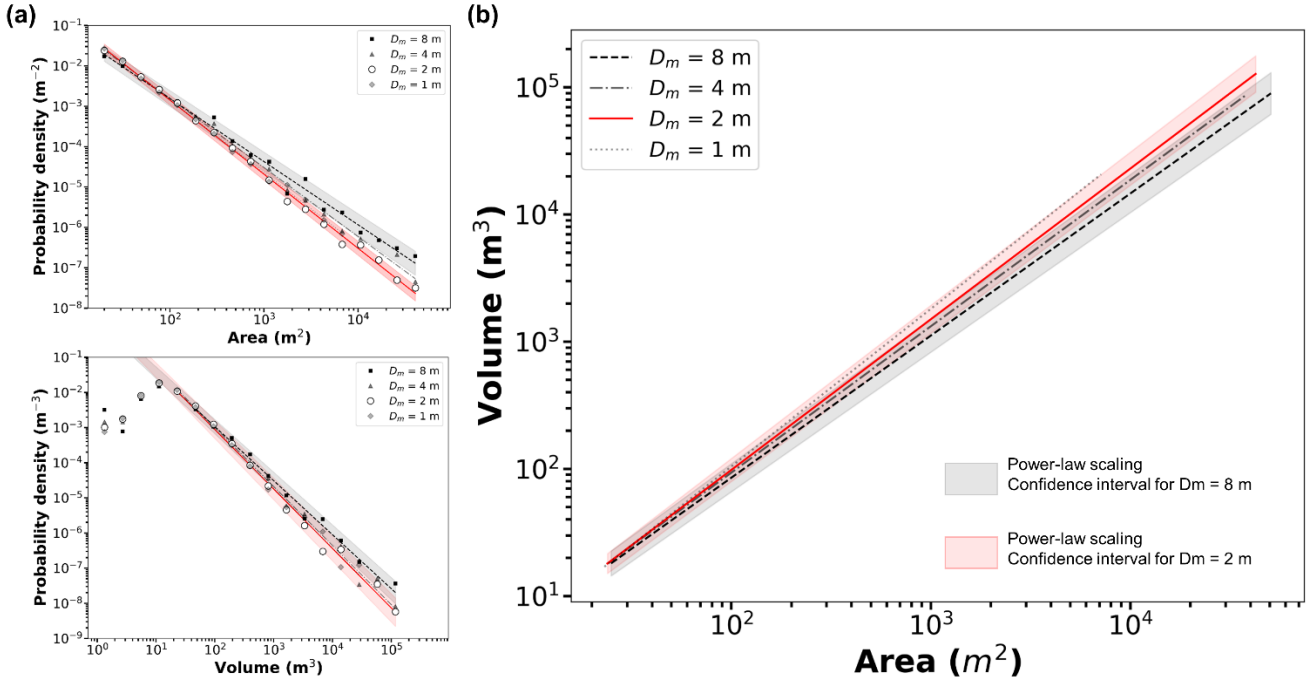

Figure S2.2.2. Sensitivity analysis of the landslide population properties for different level of segmentation. (a) Landslide area and landslide volume probability density distribution. (b) Volume-area scaling relationship. Straight lines are power-law fits of the considered parameters; values of the scaling coefficients are presented in Tab S2.

Table S2.2.2. Power-law scaling coefficients of the different level of segmentation used in the figure S4. *Dm* and NL are respectively the minimum distance between two sub-clouds and the number of landslides.

D_m (m)	N_L	Area distribution			Volume distribution			V-A relationship		
		Log a	b	R^2	Log a	b	R^2	Log α	γ	R^2
8	406	0.29 ± 0.09	-1.54 ± 0.03	0.99	0.05 ± 0.14	-1.51 ± 0.04	0.99	-0.42 ± 0.08	1.16 ± 0.02	0.99
4	938	0.61 ± 0.11	-1.70 ± 0.04	0.99	0.33 ± 0.13	-1.65 ± 0.04	0.99	-0.30 ± 0.08	1.13 ± 0.02	0.99
2	1432	0.73 ± 0.08	-1.77 ± 0.02	0.99	0.34 ± 0.10	-1.67 ± 0.03	0.99	-0.37 ± 0.08	1.18 ± 0.02	0.99
1	2083	0.76 ± 0.10	-1.79 ± 0.04	0.99	0.53 ± 0.14	-1.74 ± 0.04	0.99	-0.40 ± 0.08	1.22 ± 0.03	0.99

References

Lague, D., Brodu, N. and Leroux, J.: Accurate 3D comparison of complex topography with terrestrial laser scanner: Application to the Rangitikei canyon (N-Z), ISPRS J. Photogramm. Remote Sens., 82, 10–26, doi:10.1016/j.isprsjprs.2013.04.009, 2013.